Transcription Factors in Muscle Atrophy Caused by Blocked Neuromuscular Transmission and Muscle Unloading In Rats

Jenny Nordquist,[1] Anna-Stina Höglund,[1] Holly Norman,[1] Xiaorui Tang,[2] Barry Dworkin,[2] and Lars Larsson[1,3]

[1]Department of Neuroscience, Clinical Neurophysiology, Uppsala University, Sweden; [2]Hershey Medical Center, Hershey, Pennsylvania, USA, [3]Center for development and Health Genetics, The pennsylvania State University, University Park, USA.

The muscle wasting associated with long-term intensive care unit (ICU) treatment has a negative effect on muscle function resulting in prolonged periods of rehabilitation and a decreased quality of life. To identify mechanisms behind this form of muscle wasting, we have used a rat model designed to mimic the conditions in an ICU. Rats were pharmacologically paralyzed with a postsynaptic blocker of neuromuscular transmission, and mechanically ventilated for one to two weeks, thereby unloading the limb muscles. Transcription factors were analyzed for cellular localization and nuclear concentration in the fast-twitch muscle extensor digitorum longus (EDL) and in the slow-twitch soleus. Significant muscle wasting and upregulation of mRNA for the ubiquitin ligases MAFbx and MuRF1 followed the treatment. The IκB family–member Bcl-3 displayed a concomitant decrease in concentration, suggesting altered κB controlled gene expression, although NFκB p65 was not significantly affected. The nuclear levels of the glucocorticoid receptor (GR) and the thyroid receptor α1 (TRα1) were altered and also suggested as potential mediators of the MAFbx- and MuRF1-induction in the absence of induced Foxo1. We believe that this model, and the strategy of quantifying nuclear proteins, will provide a valuable tool for further, more detailed, analyses of the muscle wasting occurring in patients kept on a mechanical ventilator.

Online address: http://www.molmed.org
doi: 10.2119/2006–00066.Nordquist

INTRODUCTION

Skeletal muscle atrophy occurs as a consequence of many different factors, including denervation, immobilization, unloading, hormone levels, sepsis, cancer, and ageing. The effect is mediated by a shift in the normal balance between protein synthesis and protein breakdown. Knowledge about the signaling pathways involved is still scarce, but some potential molecular switches controlling the balance between hypertrophy and atrophy have been identified. Insulin-growth factor 1 (IGF-1) is one such factor, and it is believed to exert its regulatory effects via the PI3K/Akt1 pathway [reviewed in (1)]. Whereas high IGF-1/PI3K/Akt pathway activity leads to increased protein synthesis, decreased levels of IGF-1 lead to activation of proteolysis. Another factor that has been discussed in terms of both muscle growth and protein loss is H_2O_2. This highly versatile molecule mediates a variety of signals and is produced by a number of different enzyme reactions in the cells. In muscle tissue, low doses have been reported to promote myogenesis and myotube formation, whereas high doses have an opposing effect via activation of the transcription factors in the NFκB-family and an upregulation of the proteins in the ubiquitin-proteasome pathway (2,3). High H_2O_2 levels are known to be caused by increased levels of cytokines, as seen in chronic diseases, and glucocorticoid treatment and are also associated with muscle atrophy (2,4–6). A third factor that has been proposed to mediate the control of muscle size is calcineurin, a serine/threonine phosphatase that is activated in response to increased intracellular levels of Ca^{2+}. This activation is essential for the regulation of a number of transcription factors implicated in the maintenance of normal muscle functions, but its involvement in muscle hypertrophy is still a matter of debate [reviewed in (7,8)]. Nevertheless, calcineurin is a key modulator of the response to neuronal input and has been associated with muscle remodeling (9) and fiber type conversion (10).

Many signal transduction pathways linked to muscle atrophy have been associated with increased expression of two E3 ubiquitin ligases: muscle atrophy F-box (MAFbx, also known as Atrogin-1) and muscle RING finger protein 1 (MuRF1), and mice null for these genes develop less atrophy in response to denervation (11). Both MAFbx and MuRF1 gene expression have been suggested as universal markers of atrophy because they are induced by largely disparate factors such as denervation, disuse (immobilization and hindlimb suspension), treatment with a cachectic cytokine (interleukin-6), and treatment with the glucocorticoid dexamethasone (11). However, the different atrophy-inducing events have also been associated with

Address correspondence and reprint requests *to Jenny Nordquist, The Swedish Research Council, Medicine, 103 78 Stockholm Sweden; Phone: + 46 8 546 44 150; Fax: + 46 8 546 44 180 ; E-mail: Jenny.Nordquist@vr.se.*
Submitted August 23, 2006; Accepted for publication June 19, 2007.

Table 1. Transcription Factors Analyzed

Transcription factor	Family	Involved in
NFATc1	NFAT family	Activated by increased intracellular levels of Ca^{2+}. Promotes slow muscle gene program. (15).
MEF2	MADS box transcription factor	Act together with myogenin and MRF4 to sustain the muscle differentiation program (16). Binding site in mouse MyHC IIb (17).
NFκB p65 (RelA)	Subunit in the NFκB-family	Involved in muscle atrophy. Activates MuRF1 (3). The NFκB molecules are dimeric complexes containing various combinations of p50, p52, p65, RelB, and c-Rel (reviewed in (18)).
Bcl-3	IκB-family	Primarily nuclear localization. Binds p50 and p52 homodimers, which normally repress transcription. These complexes can also activate transcription (12,19).
MyoD	MRF	Skeletal muscle development. Initiation of muscle cell program. Controls expression of transcription factors, cell cycle regulators as well as muscle structural genes (reviewed in (20)).
Myogenin	MRF	Skeletal muscle development. Muscle differentiation. Mediates activity-dependent control of AchR gene expression (21).
Myf-5	MRF	Skeletal muscle development. Initiation of muscle cell program. One of the earliest markers of myogenic commitment (22).
MRF4 (Myf-6)	MRF	Skeletal muscle development. Muscle differentiation. Involved in expression of the adult Na channel (23).
Foxo1 (FKHR)	Forkhead box family	Downstream effector of the IGF-1/PI3K/Akt pathway. Reduced levels of IGF-1 activate Foxo transcription factors, which induce MuRF1 and MAFbx gene expression (24).
TRα1	Thyroid hormone receptor	Involved in determining MyHC isoforms. Tra-1-deficient mice display a switch toward more MyHC type I (25).
GR	Glucocorticoid receptor	Glucocorticoids are involved in muscle atrophy, probably via activation of GR. Can repress other transcription factors, eg, AP-1, NFκB, and Smad3 (reviewed in (26)).
Oct-1	POU homeo-domain family	Binding site in mouse MyHC IIb promoter (17,27) and possibly also in Myf-5 promoters of bovine and avian muscle (28).
Egr-3	Human zinc-finger protein	A member of the immediate-early transcription factors involved in cellular growth and differentiation. Interacts with NFκB p65 and NFAT in T cells, and controls transcription of genes encoding inflammatory cytokines (29).

variations in the response. For example, cachexia associated with disease states such as cancer and sepsis involves an increase in inflammatory cytokine production, which activates transcription factors that are, at least partly, distinct from those activated by disuse (12). How, and if, these differences affect the net result of the atrophic process is still unclear.

Muscle wasting and impaired muscle function impose a risk to critically ill ICU patients during treatment. Specifically, neuromuscular abnormalities have been reported as the dominant cause for the reduced quality of life in critically ill ICU survivors, and are remaining even up to two years after hospital discharge (13,14). Therefore, our research is focused on the molecular events mediating the muscle atrophy in ICU patients, because successful treatment of this side effect would be highly beneficial for the survival, recovery, and quality of life in these patients. To address this issue, we have used an experimental rat model mimicking the conditions for many ICU patients, such as mechanical ventilation for long durations (weeks), postsynaptic block of neuromuscular transmission to facilitate ventilation, and unloading of muscles. In this study, the levels of a number of transcription factors in nuclear extracts from muscle tissue, and their spatial organization in the muscle fiber, have been investigated. The transcription factors we selected for investigation had been implicated in the expression of MAFbx and MuRF1 or as downstream effectors of signal transduction pathways previously linked to muscle atrophy or in the regulation of differentiation and regeneration of muscle fibers. According to these criteria, we chose to analyze the basic helix-loop-helix myogenic regulatory transcription factors [MRFs: MyoD, myogenin, Myf-5, MRF4 (Myf-6)], MEF-2, NFATc1, Foxo1 (FKHR), NFκB p65, Bcl-3, thyroid receptor α1 (TRα1), glucocorticoid receptor (GR), Oct-1 and Egr-3 (Table 1). We also analyzed the mRNA levels of MAFbx and MuRF1 in these tissues. The results show that the ubiquitin ligases are upregulated, but that there are differences between fast- and slow-twitch muscles regarding the nuclear localization of a number of transcription factors, suggesting that muscles respond differently to these interventions. Differences between this experimental model and other

muscle-wasting models, including disuse and disease-associated models. are also discussed.

MATERIALS AND METHODS

Animals

Six female Sprague-Dawley rats (age 3-4 months) were anesthetized, mechanically ventilated, and treated with α-cobrotoxin for a period of 7-14 d, as previously described in detail (30). The body weight varied between 263 and 394 g (312 ± 43 g) on the first day and between 180 and 303 g (232 ± 51 g) on the final day of the experiment. Briefly, the animals were anaesthetized with isoflurane in the inspiratory gas during the surgical procedures: Precordial silver wire electrocardiogram (ECG) electrodes were implanted subcutaneously, then an abdominal aortic catheter (28-gauge Teflon) was inserted via the left femoral artery to administer parenteral solutions and to record the volume of blood pressure. A 0.9-mm Renathane catheter was threaded into the inferior vena cava from the left femoral vein, and then an ABLF21 laser Doppler flow probe was attached to the right paw. For EEG, two 0–80 screws were placed into the skull at lambda and bregma. Temperature was measured by a vaginal thermistor and servo-regulated at 37°C. A silicone cannula was inserted in the urethra to continuously record urine output.

Once the vital signs stabilized within normal limits with a continuous display of interbeat intervals, blood pressure, respiratory rate, and expired CO_2, the neuromuscular-blocking agent (NMB) α-cobrotoxin (Biotoxins, Miami, FL, USA) was injected intraarterially in rats in the NMB group. Mechanical ventilation was begun within 20–30 min, the time at which the drug begins to take effect. Neuromuscular blockade was maintained by continuous infusion of α-cobrotoxin (60 μg/day). Experiments were terminated after 7-14 d of treatment, when electrodes or other components of the preparation failed. The animals were killed while anaesthetized. In no case did animals show any signs of infections or septicemia. Untreated animals (n = 11) of the same strain and sex were included as controls.

Immediately after the rats were killed, all soleus and EDL muscles were collected immediately after euthanasia, quickly frozen in propane cooled by liquid nitrogen, and stored at –80°C for further analyses. Analysis of all muscle tissues took place simultaneously. The soleus and EDL muscles were weighed on dissection.

The Institutional Animal Care and Use Committee at the Pennsylvania State University College of Medicine approved all aspects of this study.

Preparation of Nuclear Extracts

Nuclear proteins were extracted according to a modified protocol of Dignam et al. (31). Approximately 20 mg of EDL and soleus muscles were homogenized in 1.5 mL ice-cold buffer A (10 mM HEPES, 10 mM KCl, 0.1 mM EDTA, 0.1 mM EGTA, 1 mM DTT, 0.5 mM PMSF, pH 7.9). The homogenized tissue was incubated on ice for 15 min, then 125 μL 10% nonidet P40 was added. The samples were vortexed for 10 s and subsequently centrifuged for 30 s at 13 200 rpm (Eppendorf centrifuge 5415C). The supernatant was removed and the nuclear pellet was resuspended in 400 μL buffer B (20 mM HEPES, 0.4 mM NaCl, 1 mM EDTA, 1 mM EGTA, 1 mM DTT, 1 mM PMSF, pH 7.9). The tubes were shaken vigorously for 15 min and then centrifuged at 13 200 rpm (Eppendorf centrifuge 5415C) for 5 min. The supernatant containing the nuclear proteins was aliquoted and frozen at –80 °C. All the steps described above were performed at 4 °C. The total protein concentration was quantified using the BCA Protein Assay kit from Pierce (Pierce, Rockford, IL, USA).

Enzyme-Linked Immunosorbent Assay

Microtiter plates (96-well) were coated with 50 μL nuclear extracts diluted 1:150 in 50 mM carbonate-bicarbonate buffer, pH 9.0, to an approximate concentration of 2 μg/mL total protein. The plates were covered with parafilm and incubated overnight at 4 °C. After the incubation, the antigen solution was removed and 200 μL blocking buffer (PBS, 1% BSA) was added. The plates were incubated for one hour in room temperature and were thereafter washed six times with wash buffer I (PBS with 0.05% Tween 20), then 50 μL primary antibody (15 μg/mL, rabbit polyclonal) diluted in blocking buffer was added to each well. The plates were incubated overnight in a humidified chamber at 4 °C. After the incubation, the antibody was removed, the plates were washed, and 50 μL of secondary antibody was added (1.14 μg/mL, AP-conjugated chicken anti-rabbit; Santa Cruz Biosciences, Santa Cruz, CA, USA). After incubation for two hours at room temperature, the plates were washed six times with wash buffer I and once with wash buffer II (10 mM diethanolamine, 0.5 mM $MgCl_2$, pH 9.5). Thereafter, 50 μL of the AP-substrate (phosphate substrate, 5 mg tablet diluted in wash buffer II; Sigma, St. Louis, MO, USA) was added to each well. The enzyme-reaction was terminated after 10-20 min by the addition of 50 μL 0.1 M EDTA, pH 7.5, to each well. The plates were analyzed in a microplate reader (Labsystems iEMS Reader MF) at OD 405 nm.

All primary antibodies were from SantaCruz biosciences: Bcl-3 (sc-185), Egr-3 (sc-191), Foxo1 (sc-11350), GR (sc-8992), MEF-2 (sc-313), Myf-5 (sc-302), Myf-6 (sc-301), MyoD (sc-304), Myogenin (sc-576), NFATc1 (sc-13033), NFκB p65 (sc109), Oct-1 (sc-232), and TRα1 (sc-772). The antibodies were tested for specificity using Western blot, and were found to be acceptable for our analyses in that they displayed one band in the expected molecular weight range. TRα1, however, was not detectable using Western blot and could thus not be evaluated. Some ambiguity was observed regarding Bcl-3 and NFκB p65, both of which showed several bands, presumably relating to homo- or heterodimers with other NFκB subunits. In addition, Foxo1 displayed two bands, possibly as a result of degradation.

Table 2. Primers Used for Real-Time RT-PCR

Gene	Primer sequences	Product (bp)
MAFbx	Forward 5´ TCCTGGATTCCAGAAGATTCAAC 3´ Reverse 5´ TCAGGGATGTGAGCTGTGACTT 3´	75
MuRF1	Forward 5´ ACAACCTCTGCCGGAAGTGT 3´ Reverse 5´ CCGCGGTTGGTCCAGTAG 3´	67
18S	Forward 5´ GTGCATGGCCGTTCTTAGTTG 3´ Reverse 5´ AGCATGCCGAGAGTCTCGTT 3´	74

Real-Time RT-PCR

Primers for MAFbx (GenBank accession AY059628), MuRF1 (GenBank accession AY059627), as well as 18S ribosomal RNA (GenBank accession AF102857) were designed using the software Primer Express® (Applied Biosystems, Foster City, CA, USA). HPLC-purified primers were purchased from Thermo Electron GmBH (Ulm, Germany). Sequences for the primers are listed in Table 2. BLAST-searches revealed no cross-reactivity toward any other DNA sequences in rat.

RNA purification, cDNA synthesis, and PCR (run on an MyiQ™ instrument; BioRad, Hercules, CA, USA) were performed as described previously (32). Threshold cycle (C_T) data obtained from running real-time RT-PCR was related to a standard curve to obtain the starting quantity (SQ) of the template cDNA, and the values were normalized against 18S rRNA (32).

Immunohistochemistry

Sections cut from EDL and soleus muscles were stained using the same primary antibodies as described above for the enzyme-linked immunosorbent assay (ELISA). In addition to the antibodies against transcription factors, some sections were costained with a mouse antibody against type I myosin heavy chain (MyHC) (33). Briefly, cryosections were fixed in 3.7% formaldehyde in PBS for 20 min, and subsequently blocked in 1% BSA in PBS for 30 min. Primary antibodies diluted 1:50 in blocking buffer (4 μg/mL final concentration) were then added, and the slides were incubated for one hour at room temperature. After this step, the sections were incubated with fluorescently labeled secondary antibodies (2 μg/mL final concentration) for 30 min. The secondary antibodies were goat anti-mouse IgG conjugated with Alexa fluor 633 and goat anti-rabbit IgG conjugated with Alexa fluor 488 (Molecular Probes, Invitrogen, Carlsbad, CA, USA). Finally, all nuclei were stained using 1:1000 dilution of DAPI (Molecular Probes). The sections were thoroughly washed in PBS between all the different incubations and finally mounted in polyvinyl alcohol mounting medium (Fluka Biochemika, Buchs. Switzerland). All slides contained negative control sections without primary antibody, to ensure the specificity of the staining. Acquisition of these images was made under conditions identical to the respective primary/secondary antibody staining. The Alexa 488–conjugated secondary antibody showed almost no background fluorescence, whereas the Alexa 633–conjugated secondary antibody showed a slight staining between the individual muscle cells. For the studies on localization of individual transcription factors within the sarcomere, rhodamine-labeled phalloidin was used to stain the actin, and in these cases we also included negative controls without the primary antibody.

Images were taken with a Zeiss confocal microscope, LSM 510 Meta, using the laser diode 405, the argon laser 488 and HeNe lasers for 543 and 633 respectively. Filter settings were as follows; BP 420-480 nm, BP 505-530 nm, BP560-615, and for the meta channel S1 650-750. Images

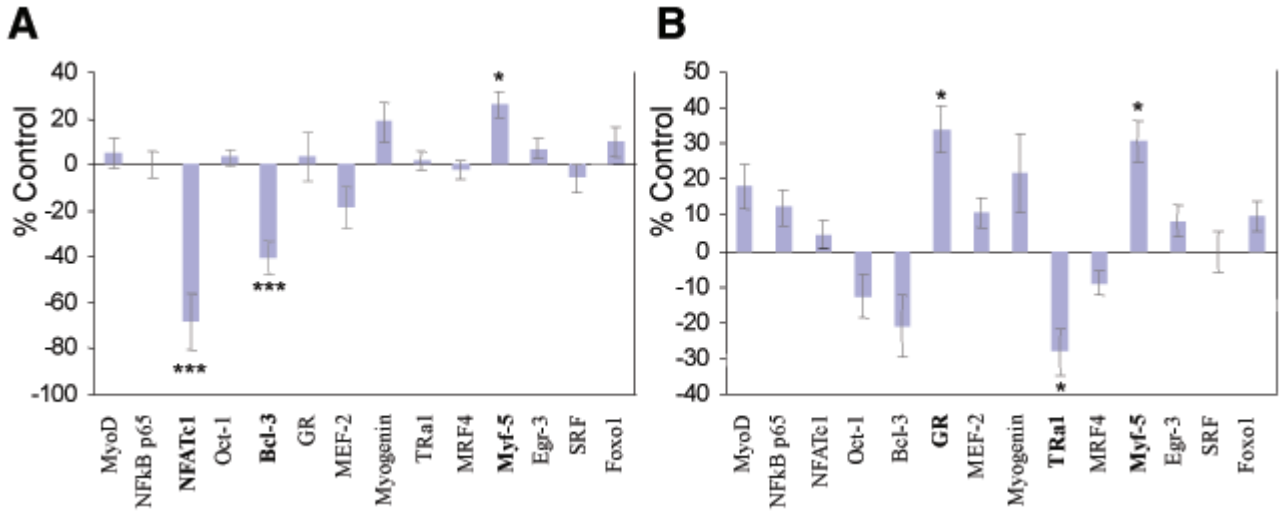

Figure 1. Transcription factors quantified in nuclear extracts using ELISA. The bars represent the relative change for NMB as a percentage of control in A. EDL and B. Soleus. *$P < 0.05$, ***$P < 0.001$. Error bars represent SEM.

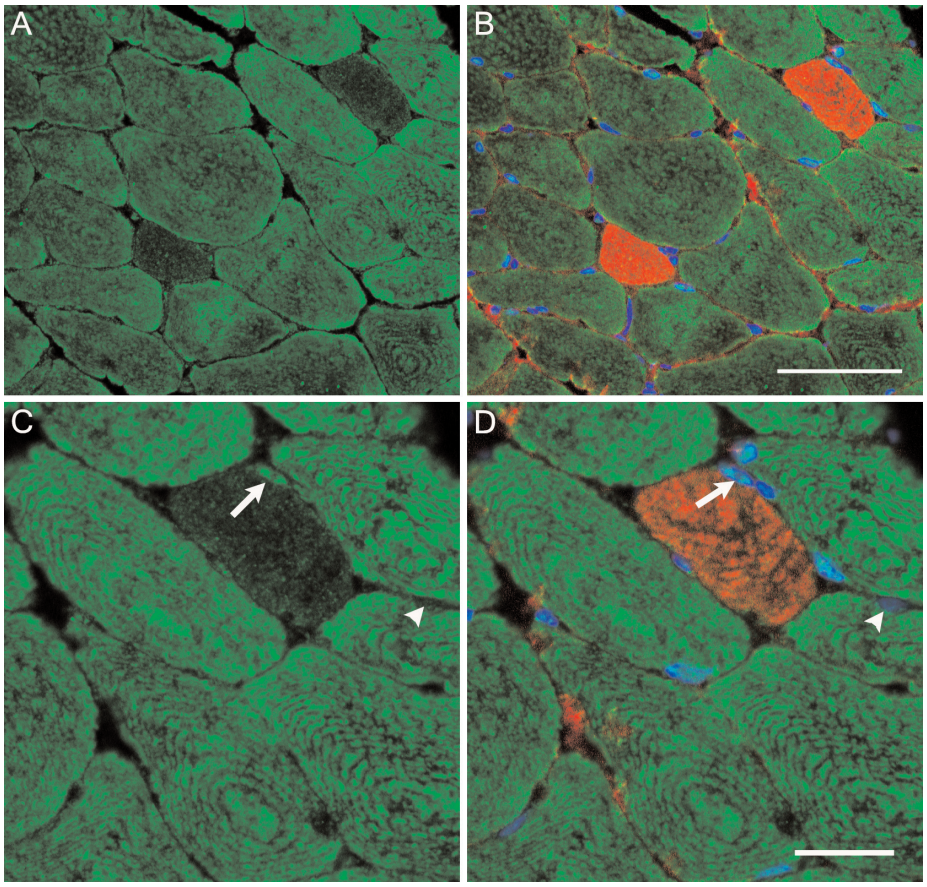

Figure 2. Cross sections of EDL muscle from an NMB rat showing Myf-5 (green), MyHC type I (red) and nuclei (blue). Myf-5 shows a clear nuclear localization and a predominant staining in the cytoplasm of type II fibers. (A) Myf-5 staining only, (B) composite view of all fluorophores, scale bar 50 μm. A higher magnification of the area in (A) and (B) is shown in (C) and (D). Some nuclei are intensely stained for Myf-5 (arrows) while it is absent in others (arrowhead), scale bar 20 μm.

were taken with a plan neofluar 20x/0.5 and C-apochromat 40x/1.2W.

Statistics

Mean and standard deviation (SD) of means were calculated, and groups were compared using the Student unpaired t-test. When the normality test failed, a nonparametric Mann-Whitney rank sum test was performed. The results were considered to be statistically significant when $P < 0.05$.

RESULTS

Muscle Size

The muscle mass was lower in both EDL and soleus of NMB compared with controls (96 ± 24 mg versus 131 ± 20 mg, $P < 0.01$; and 74 ± 14 mg versus 126 ± 17 mg, $P < 0.001$, respectively), and there was a trend toward lower body weight (243 ± 55 g versus 319 ± 67 g, $P = .09$).

Quantification of Nuclear Proteins

There was a trend toward a reduction in total protein concentration in the nuclear extracts from soleus (223 ± 68 μg/mL compared with control, 315 ± 96 μg/mL, $P = .054$). Despite this trend, we used the total protein in these samples as a normalizing factor when quantifying specific nuclear proteins. A normalizing factor is essential for correcting variations in the extraction process, and by using total protein for this purpose we obtained valuable information as to whether a specific protein is reduced, spared, or/increased compared with the complete pool of protein in the sample.

The quantification of transcription factors in the nuclear extracts (ELISA) showed that the response to NMB differed to some extent between EDL and soleus muscles (Figure 1). Most strikingly, NFATc1 was reduced by 70% in the EDL ($P < 0.001$), but was not significantly affected in the soleus of the NMB rats. Also TRα1, GR and Bcl-3 displayed clear differences between the two muscles. The levels of TRα1 were reduced by 28% and GR was increased by 34% in the soleus ($P < 0.05$), whereas their respective levels in EDL were not affected. Bcl-3, on the other hand, was reduced in the EDL ($P < 0.001$), but was not significantly changed in the soleus.

All other proteins analyzed reacted similarly in EDL and soleus. Most of them did not display altered concentrations, such as MyoD, myogenin, MRF4, MEF-2, Foxo1, NFκB p65, Oct-1 and Egr-3. Myf-5, on the other hand, was increased in both EDL and soleus compared with the controls ($P < 0.05$).

Immunohistochemistry

The cellular localization of the different transcription factors was analyzed by costaining the tissue sections with antibodies against the β/slow (type I) MyHC and by staining the nuclei with DAPI. The ELISA used for a quantitative analysis, had shown that the responses in EDL and soleus differed for some transcription factors (above), and this was hypothesized to be due to the disparate fiber-type composition of the two muscles. The fast-twitch EDL is predominantly composed of fibers expressing type II MyHC isoforms, whereas soleus is mainly composed of slow type I fibers. Thus, one objective of using immunohistochemistry was to analyze any differences between fiber types regarding localization and occurrence of these transcription factors. The most striking differences were observed in the cytoplasm between the different fiber types.

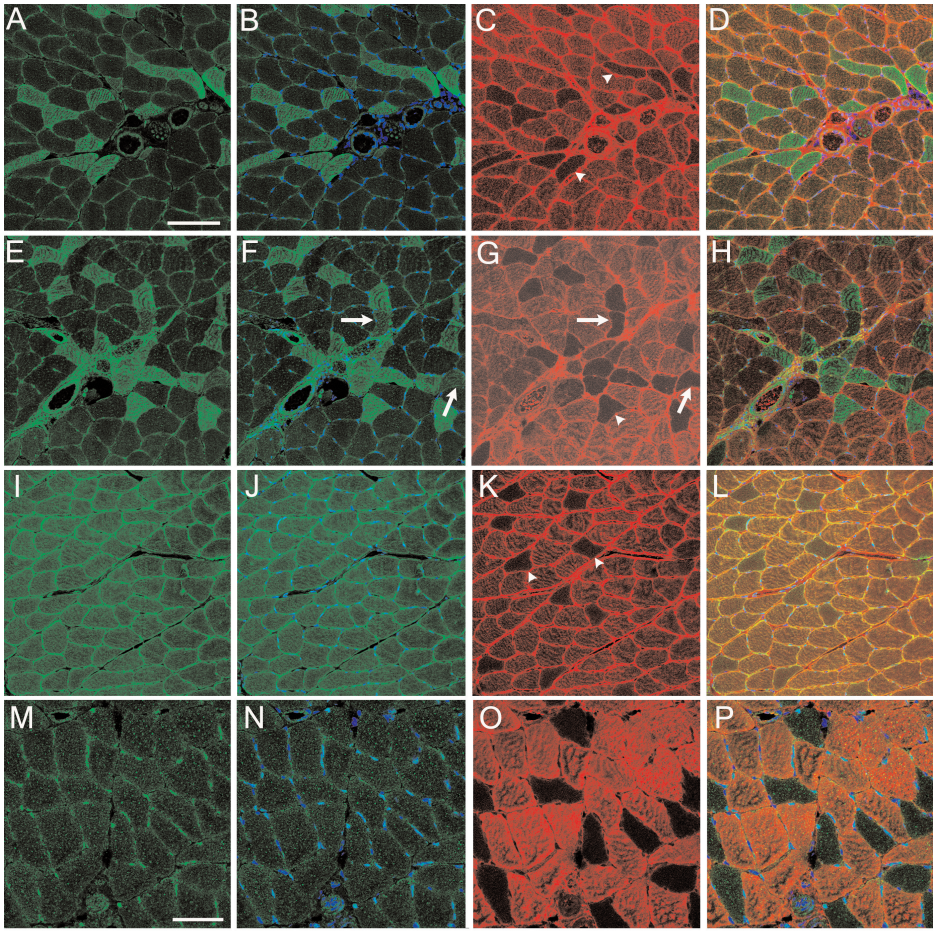

Figure 3. Cross sections of soleus muscle. (A), (E), (I), and (M) show the localization of glucocorticoid receptor, NFκB, MEF-2, and Myogenin, respectively. In (B), (F), (J), and (N) the nuclei are displayed together with respective transcription factors. In (C), (G), (K), and (O), corresponding images display the type I fibers in red and type II fibers unstained (some marked by arrowheads). The NFκB concentration appears with different intensity among the type II fibers (areas of less intensity are indicated by arrows). The scale bar for A–L is 100 μm and the scale bar for M–P is 50 μm.

GR and Myf-5 displayed a clear predominance in the cytoplasm of type I-negative fibers, leaving the cytoplasm of type I fibers practically devoid of these transcription factors (Figure 2). NFκB p65, on the other hand, showed a large heterogeneity among the type I–negative fibers. In no case, however, were we able to visualize any differences between type I– and type I–negative fibers regarding the nuclear localization of transcription factors (Figure 3).

Because NFATc1 was the most significantly downregulated protein in the nuclear extracts, we expected a visible reduction in its nuclear localization. However, although the quantifications obtained with ELISA showed a clear reduction of NFATc1 in the nuclei of NMB EDL, with only about 30% of the control levels remaining, we could not detect such a change in our confocal images. Nor could we detect a difference between type I and type II fibers (Figure 4B-D). In fact, the most striking finding was the intense staining of NFATc1 in vascular smooth muscle compared with skeletal muscle (Figure 4A).

In longitudinal sections we observed that all transcription factors analyzed displayed a striated pattern (Figure 4A). A double staining performed to visualize actin (using rhodamin phalloidin) and respective transcription factor revealed that MyoD, NFκB p65, Oct-1, Bcl-3, GR, MRF-4, and NFATc1 were located between the actin bands, whereas MEF-2, Myogenin, TRα1, Egr-3, and Foxo-1 seemed to at least partially colocalize to the actin bands (not shown).

mRNA Quantification

The mRNA levels of the ubiquitin ligases MAFbx and MuRF1, as well as 18S rRNA, were analyzed using real-time RT-PCR. The 18S rRNA was confirmed to be unaffected by the treatment and could thus serve as an internal control [EDL: SQ 1.02 ± 0.28 in NMB versus SQ 0.73 ± 0.38 in controls, not significant (NS); and soleus: SQ 2.36 ± 1.09 in NMB versus SQ 2.32 ± 0.70 in controls, NS]. Both MuRF1 and MAFbx were significantly upregulated in both EDL ($P < 0.05$ and $P < 0.01$, respectively) and soleus ($P < 0.001$ and $P < 0.05$, respectively) (Figure 5).

DISCUSSION

In muscle atrophy, the balance between protein synthesis and degradation is shifted. The objective of this study was to analyze some of the transcription factors that control muscle size, and how they were affected in our rodent ICU muscle-wasting model.

Protease-Inducing Pathways

The ubiquitin ligases MAFbx and MuRF1 were upregulated in the NMB rats (Figure 5), which is in accordance with other models of muscle atrophy, including dexamethasone- (glucocorticoid) or interleukin-1–induced wasting, hindlimb suspension, and denervation (11). The unchanged nuclear levels of Foxo1, considered a modifier of MAFbx and MuRF1 activities, as well as of NFκB p65, which has been implicated in MuRF1 activation (3), were therefore unexpected and suggest an alternative upregulation of MAFbx and MuRF1 in this ICU model of muscle wasting. The lack of activation of these transcription factors has to be cautiously interpreted because the animals were all exposed to

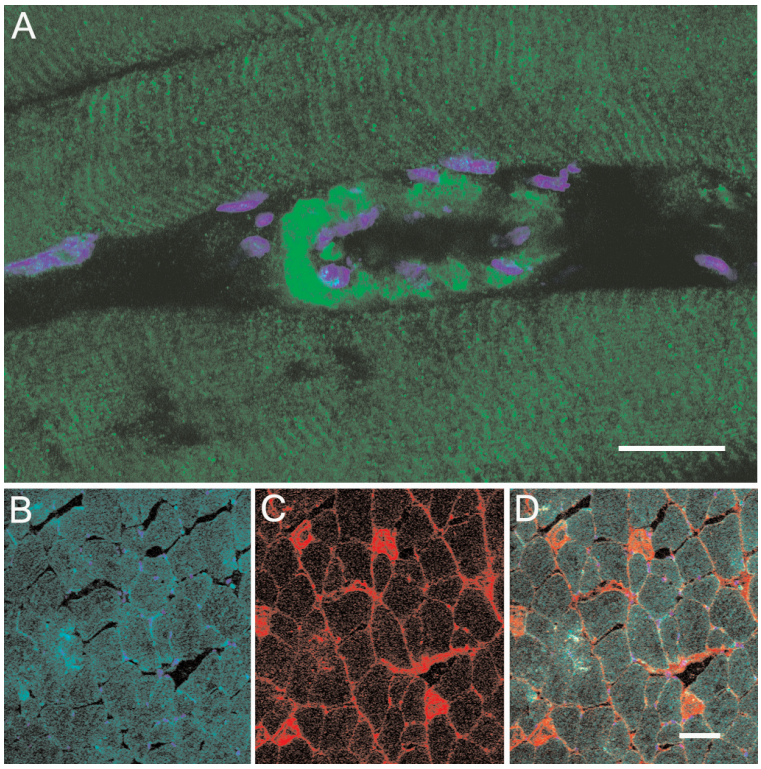

Figure 4. (A) Localization of NFATc1 (green) in a longitudinal section of EDL muscle from a control rat. A faint staining of nuclei and cytoplasm is visible in the muscle fibers. Note also the striated pattern suggesting an association of NFATc1 to sarcomeric proteins. The most intense staining is found in the vascular smooth muscle cells. (B–D) Cross section of EDL muscle from a control rat. (B) Localization of NFATc1 is shown in green and nuclei in blue; (C) distribution of type I fibers (red); (D) composite image. Scale bar for A is 20 μm and for B–D 50 μm.

long-term treatment, and thus transient or early responses may pass undetected. Nevertheless, in EDL the large reduction of Bcl-3 must be considered a potential mediator of such an alternative or complementary mechanism. Bcl-3 is an IκB family member, and it possesses dual functions in transcription. Bcl-3 can bind to p50 and p52 homodimers (members of the NFκB family), which normally act as transcriptional repressors, and, depending on the Bcl-3 concentration and phosphorylation, either remove or enhance their binding to κB sites (34). Additionally, the Bcl-3 complexes with p50 and p52 homodimers can also act as transactivators [reviewed in (35)]. Thus, the reduction of Bcl-3 in EDL is likely to have an impact on κB controlled gene expression, and MuRF1 has been shown to be one such gene (3). Increased levels of Bcl-3 have previously been reported in disuse-induced muscle wasting (12), but to our knowledge there have been no reports on decreased levels. It is therefore possible that this response is unique for our ICU muscle-wasting model.

In soleus, the levels of Bcl-3 were not significantly decreased in NMB rats. On the other hand, increased levels of GR and decreased levels of TRα1 were observed in the soleus, and both of these findings may represent mechanisms alternative or complementary to NFκB p65—or Foxo 1—induced MAFbx and MuRF1 expression. Previous studies have linked increased levels of both glucocorticoids and thyroid hormone to increased levels of ubiquitin ligases (36,37), but decreased levels of thyroid hormone have also been linked to muscle wasting [reviewed in (38)]. In addition to the association with ubiquitin ligases, glucocorticoids have also been associated with an upregulation of myostatin, which is a negative regulator of muscle mass (39). As for TR deficiency, it has been implicated in a shift toward a slow MyHC phenotype, both in soleus and EDL (25), and is thus involved in the synthesis of myosin, but the mechanisms underlying atrophy in hypothyroidism remain poorly understood.

Pathways in Protein Synthesis

The NMB rats have previously been analyzed for mRNA levels of MyHC isoforms and actin, as well as myosin-binding proteins. We observed a general downregulation of all these transcripts, except for myosin-binding protein H, indicating that the muscle wasting in the ICU is associated with a decreased protein synthesis (32). In addition to the lowered levels of TRα1, which has a role in myosin isoform switching (above), we have also identified NFATc1 as a potential mediator of the reduced transcription. The nuclear localization of NFATc1 as a response to increased intracellular levels of Ca^{2+} and activation of calcineurin, electrical stimuli, and neuronal input has been described extensively, and the results indicate that this localization is important for driving the muscle fibers toward a slow phenotype (15,40,41). In the present study, we found decreased levels of NFATc1 in EDL nuclear extracts as a response to NMB, whereas the levels in soleus were constant, a pattern that we have also observed in denervated animals (Nordquist et al., unpublished data). The reason for this finding is unclear, but it suggests that NMB (and denervation) have a stronger effect on NFATc1-controlled gene expression in fast-twitch fibers. This explanation, however, is not in accordance with results from Tothova et al., who found a more pronounced effect on the slow-twitch soleus compared with the fast-twitch tibialis anterior (42). This discrepancy may be due to differences in the experimental set-up and time-span of the

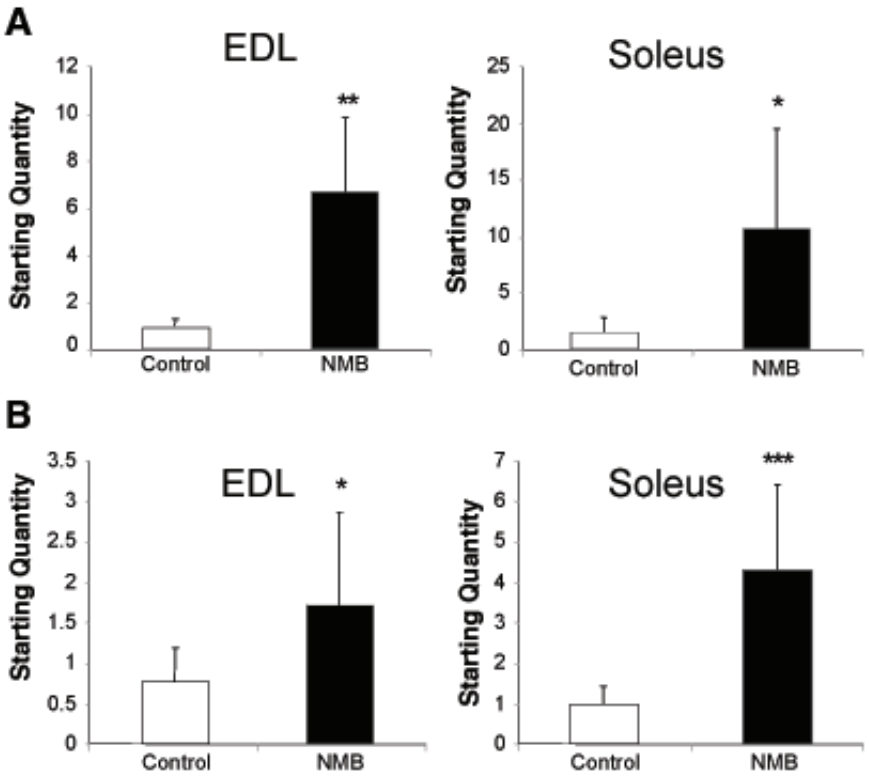

Figure 5. mRNA levels of MuRF1 (A) and MAFbx (B) in EDL and soleus muscle tissues. NMB, n = 4; controls, n = 8. *$P < 0.05$, **$P < 0.01$, ***$P < 0.001$.

studies, but we also need to address the contribution from vascular smooth muscle in our nuclear preparations because this tissue has a very high concentration of NFATc1 compared with skeletal muscle tissue (Figure 4A). This finding raises the question as to whether NMB (and denervation) also affect vascular tissue, and if so, if the vascular tissue in EDL would be more affected than that in the soleus.

The nuclear levels of Myf-5 were increased in both EDL and soleus. Being one of the earliest markers of myogenic commitment, Myf-5 is expressed in satellite cells and is further induced as the satellite cells are activated (22,43). This process is normally followed by an induction of MyoD as the satellite cells exit the cell cycle and start to differentiate (44). Considering that we observed no induction of MyoD, the satellite cells may be activated, but are not likely to be differentiating in the NMB animals. However, Myf-5 is also present in the cytoplasm of type II myofibers and in the myonuclei, and therefore it is possible that this transcription factor is increased to counteract the atrophic process and to maintain the myogenic phenotype. Myf-5 could also be a marker of an isoform switch toward more type II fibers.

Cellular Localization of Transcription Factors

The striated pattern for all transcription factors analyzed suggests an association to sarcomeric proteins. NFAT has previously been reported to be associated with the Z-disc (40), possibly via the calcineurin-interacting proteins, the calsarcins (45). Although the importance of the sarcomeric localization for transcriptional control is not known, it is tempting to speculate that it represents a link between mechanical strain and gene expression. The transcription factor SRF has previously been linked to such a pathway, which is initiated when a kinase domain in titin is activated due to a mechanically induced conformational change of the protein (46).

The fact that GR and Myf-5 displayed a clear predominance in the cytoplasm of type II fibers is interesting and warrants further investigations, as does the variable occurrence of NFκB p65 in type II fibers. To our knowledge, these transcription factors have not been implicated in fiber-type specific transcription, but the present results indicate that they may play a role in determining a fast- or slow-twitch phenotype. GR and Myf-5 are increased in soleus muscles from the NMB rats, a finding indicating that these factors may be markers of, or actively involved in, the driving of an isoform switch toward more type II fibers in these tissues.

Experimental Set-Up

The dramatic loss of body weight, muscle mass in particular, generally observed in critically ill mechanically ventilated ICU patients was confirmed in our experimental ICU model. In fact, the muscle wasting observed after nine days in this model exceeded the loss in muscle mass observed after three weeks of peripheral denervation or four weeks cast immobilization (47,48). The absence of muscle membrane depolarization in combination with muscle unloading have, accordingly, a very strong negative effect on muscle mass that goes beyond what is observed after denervation, immobilization, or disuse.

Thus, the rodent ICU muscle-wasting model used in this study has several similarities with modern intensive care treatment, such as mechanical ventilation, blocked neuromuscular transmission, and muscle unloading, but without the confounding influence of differences in systemic disease and pharmacological treatment. The results from this study and a previous study focusing on myofibrillar protein and mRNA expression (32) have documented the usefulness of this model for future and more detailed studies of muscle wasting in ICU patients. The model enables time-resolved

studies, as well as studies regarding mechanical ventilation, neuromuscular blockade, muscle unloading, and corticosteroid treatment separately and in different combinations. Furthermore, some ICU patients are afflicted by a more aggressive form of atrophy, known as critical illness myopathy or acute quadriplegic myopathy, which is an acute paralysis of all spinal nerve–innervated muscles and a partial or complete depletion of myosin and myosin-associated thick filament proteins, and it is our ambition to use the rat model presented here to study this disease.

Summary

The rat ICU model presented here displays some characteristics previously not associated with other atrophy-inducing models. The major findings include: (*a*) Bcl-3, GR, and TRα1 are possible candidates for mediating ICU-induced muscle wasting. (*b*) Myf-5-induction occurred, resulting either from satellite cell activation or from an isoform shift in MyHC toward more type II fibers, or a combination thereof. An isoform shift is also an alternative explanation for the increased GR levels in soleus, because GR is also predominantly expressed in the cytoplasm of type II fibers. (*c*) NFATc1 was mainly found in vascular smooth muscle tissue, and the specific reduction in EDL must therefore also be considered in terms of vascular effects.

By using this directed-screening approach, our goal is to obtain a better understanding of the processes leading to muscle wasting in ICU patients. Knowledge about such underlying mechanisms is essential for correct diagnosis and the design of specific intervention strategies.

ACKNOWLEDGMENTS

We wish to thank Yvette Hedström, Helena Svahn, and Ann-Marie Gustafson for excellent technical assistance. The study was supported by grants from the Medical Faculty´s Foundation for Psychiatric and Neurological Research at Uppsala University to J.N., and the Swedish Research Council (08651), NIH (AR045627, AR047318, AG014731), Association Française contre les Myopathies (AFM), and the Swedish Cancer Society, to L.L.

REFERENCES

1. McKinnell IW, Rudnicki MA. (2004) Molecular mechanisms of muscle atrophy. *Cell* 119:907–10.
2. Orzechowski A, Grizard J, Jank M, Gajkowska B, Lokociejewska M, Zaron-Teperek M Godlewski, M. (2002) Dexamethasone-mediated regulation of death and differentiation of muscle cells: Is hydrogen peroxide involved in the process? *Reprod. Nutr. Dev.* 42:197–216.
3. Cai D, Frantz JD, Tawa NE, et al. (2004) IKKbeta/NF-kappaB activation causes severe muscle wasting in mice. *Cell* 119:285–98.
4. Li YP, Chen Y, John J, Moylan J, Jin B, Mann DL, Reid MB. (2005) TNF-alpha acts via p38 MAPK to stimulate expression of the ubiquitin ligase atrogin1/MAFbx in skeletal muscle. *FASEB. J.* 19:362–70.
5. Gomes-Marcondes MC, Tisdale MJ. (2002) Induction of protein catabolism and the ubiquitin-proteasome pathway by mild oxidative stress. *Cancer Lett*. 180:69–74.
6. Li YP, Chen Y, Li AS, Reid MB. (2003) Hydrogen peroxide stimulates ubiquitin-conjugating activity and expression of genes for specific E2 and E3 proteins in skeletal muscle myotubes. *Am. J. Physiol. Cell Physiol*. 285:C806–12.
7. Michel RN, Dunn SE, Chin ER. (2004) Calcineurin and skeletal muscle growth. *Proc. Nutr. Soc*. 63:341–9.
8. Schiaffino S, Serrano A. (2002) Calcineurin signaling and neural control of skeletal muscle fiber type and size. *Trends Pharmacol. Sci*. 23:569–75.
9. Sakuma K, Nishikawa J, Nakao R, et al. (2003) Calcineurin is a potent regulator for skeletal muscle regeneration by association with NFATc1 and GATA-2. *Acta. Neuropathol. (Berl.)* 105:271–80.
10. Chin ER, Olson EN, Richardson JA, et al. (1998) A calcineurin-dependent transcriptional pathway controls skeletal muscle fiber type. *Genes Dev*. 12:2499–509.
11. Bodine SC, Latres E, Baumhueter S, et al. (2001) Identification of ubiquitin ligases required for skeletal muscle atrophy. *Science* 294:1704–8.
12. Hunter RB, Stevenson E, Koncarevic A, Mitchell-Felton H, Essig DA, Kandarian SC. (2002) Activation of an alternative NF-kappaB pathway in skeletal muscle during disuse atrophy. *FASEB J.* 16:529–38.
13. Herridge MS, Cheung AM, Tansey CM, et al. (2003) One-year outcomes in survivors of the acute respiratory distress syndrome. *N. Engl. J. Med*. 348:683–3.
14. Cheung AM, Tansey CM, Tomlinson G, et al. (2006) Two-year outcomes, health care use and costs in survivors of ARDS. *Am. J. Respir. Crit. Care Med*. 174:538–44.
15. Kubis HP, Hanke N, Scheibe RJ, Meissner JD, Gros G. (2003) Ca2+ transients activate calcineurin/NFATc1 and initiate fast-to-slow transformation in a primary skeletal muscle culture. *Am. J. Physiol. Cell Physiol*. 285:C56-63.
16. Molkentin JD, Black BL, Martin JF, Olson EN. (1995) Cooperative activation of muscle gene expression by MEF2 and myogenic bHLH proteins. *Cell* 83:1125–36.
17. Lakich MM, Diagana TT, North DL, Whalen RG. (1998) MEF-2 and Oct-1 bind to two homologous promoter sequence elements and participate in the expression of a skeletal muscle-specific gene. *J. Biol. Chem*. 273:15217–26.
18. Schmitz ML, Mattioli I, Buss H, Kracht M. (2004) NF-kappaB: a multifaceted transcription factor regulated at several levels. *Chembiochem*. 5: 1348–58.
19. Heissmeyer V, Krappmann D, Wulczyn FG, Scheidereit C. (1999) NF-kappaB p105 is a target of IkappaB kinases and controls signal induction of Bcl-3-p50 complexes. *Embo. J*. 18:4766–78.
20. Berkes CA, Tapscott SJ. (2005) MyoD and the transcriptional control of myogenesis. *Semin. Cell Dev. Biol*. 16:585–95.
21. Tang H, Macpherson P, Argetsinger LS, Cieslak D, Suhr ST, Carter-Su C, Goldman D. (2004) CaM kinase II-dependent phosphorylation of myogenin contributes to activity-dependent suppression of nAChR gene expression in developing rat myotubes. *Cell. Signal*. 16:551–63.
22. Tajbakhsh S, Buckingham M. (2000) The birth of muscle progenitor cells in the mouse: spatiotemporal considerations. *Curr. Top. Dev. Biol*. 48: 225–68.
23. Thompson AL, Filatov G, Chen C, Porter I, Li Y, Rich MM, Kraner SD. (2005) A selective role for MRF4 in innervated adult skeletal muscle: Na(V) 1.4 Na+ channel expression is reduced in MRF4-null mice. *Gene Expr*. 12:289–303.
24. Stitt TN, Drujan D, Clarke BA, et al. (2004) The IGF-1/PI3K/Akt pathway prevents expression of muscle atrophy-induced ubiquitin ligases by inhibiting FOXO transcription factors. *Mol. Cell* 14:395–403.
25. Yu F, Gothe S, Wikstrom L, Forrest D, Vennstrom B, Larsson L. (2000) Effects of thyroid hormone receptor gene disruption on myosin isoform expression in mouse skeletal muscles. *Am. J. Physiol. Regul. Integr. Comp. Physiol*. 278: R1545–54.
26. Schacke H, Docke WD, Asadullah K. (2002) Mechanisms involved in the side effects of glucocorticoids. *Pharmacol. Ther*. 96:23–43.
27. Allen DL, Weber JN, Sycuro LK, Leinwand LA. (2005) Myocyte enhancer factor-2 and serum response factor binding elements regulate fast Myosin heavy chain transcription in vivo. *J. Biol. Chem*. 280:17126–34.
28. Barth JL, Morris J, Ivarie R. (1998) An Oct-like binding factor regulates Myf-5 expression in primary avian cells. *Exp. Cell Res*. 238:430–8.
29. Wieland GD, Nehmann N, Muller D, et al. (2005) Early growth response proteins EGR-4 and

EGR-3 interact with immune inflammatory mediators NF-kappaB p50 and p65. *J. Cell. Sci.* 118: 3203–12.
30. Dworkin BR, Dworkin S, Tang X. (2000) Carotid and aortic baroreflexes of the rat: I. Open-loop steady-state properties and blood pressure variability. *Am. J. Physiol. Regul. Integr. Comp. Physiol.* 279:R1910–21.
31. Dignam JD, Lebovitz RM, Roeder RG. (1983) Accurate transcription initiation by RNA polymerase II in a soluble extract from isolated mammalian nuclei. *Nucleic Acids Res.* 11:1475–89.
32. Norman H, Nordquist J, Andersson P, Ansved T, Tang X, Dworkin B, Larsson L. (2006) Impact of post-synaptic block of neuromuscular transmission, muscle unloading and mechanical ventilation on skeletal muscle protein and mRNA expression. *Pflugers Arch.* 453:53-66.
33. Hughes SM, Cho M, Karsch-Mizrachi I, Travis M, Silberstein L, Leinwand LA, Blau HM. (1993) Three slow myosin heavy chains sequentially expressed in developing mammalian skeletal muscle. *Dev. Biol.* 158:183–99.
34. Bundy DL, McKeithan TW. (1997) Diverse effects of BCL3 phosphorylation on its modulation of NF-kappaB p52 homodimer binding to DNA. *J. Biol. Chem.* 272:33132–9.
35. Bates PW, Miyamoto S. (2004) Expanded nuclear roles for IkappaBs. *Sci. STKE 2004.* pe48
36. Sultan KR, Henkel B, Terlou M, Haagsman HP. (2006) Quantification of hormone-induced atrophy of large myotubes from C2C12 and L6 cells: atrophy-inducible and atrophy-resistant C2C12 myotubes. *Am. J. Physiol. Cell. Physiol.* 290: C650–9.
37. Clement K, Viguerie N, Diehn M, et al. (2002) In vivo regulation of human skeletal muscle gene expression by thyroid hormone. *Genome Res.* 12: 281–91.
38. Rooyackers OE, Nair KS. (1997) Hormonal regulation of human muscle protein metabolism. *Annu. Rev. Nutr.* 17:457–85.
39. Ma K, Mallidis C, Bhasin S, et al. (2003) Glucocorticoid-induced skeletal muscle atrophy is associated with upregulation of myostatin gene expression. *Am. J. Physiol. Endocrinol. Metab.* 285: E363–71.
40. Liu Y, Cseresnyes Z, Randall WR, Schneider MF. (2001) Activity-dependent nuclear translocation and intranuclear distribution of NFATc in adult skeletal muscle fibers. *J. Cell Biol.* 155:27–39.
41. McCullagh KJ, Calabria E, Pallafacchina G, et al. (2004) NFAT is a nerve activity sensor in skeletal muscle and controls activity-dependent myosin switching. *Proc. Natl. Acad. Sci. U S A* 101: 10590–5.
42. Tothova J, Blaauw B, Pallafacchina G, Rudolf R, Argentini C, Reggiani C, Schiaffino S. (2006) NFATc1 nucleocytoplasmic shuttling is controlled by nerve activity in skeletal muscle. *J. Cell. Sci.* 119:1604-11.
43. Zammit PS, Heslop L, Hudon V, et al. (2002) Kinetics of myoblast proliferation show that resident satellite cells are competent to fully regenerate skeletal muscle fibers. *Exp. Cell Res.* 281: 39–49.
44. Beauchamp JR, Heslop L, Yu DS, et al. (2000) Expression of CD34 and Myf5 defines the majority of quiescent adult skeletal muscle satellite cells. *J. Cell Biol.* 151:1221–34.
45. Frey N, Richardson JA, Olson EN. (2000) Calsarcins, a novel family of sarcomeric calcineurin-binding proteins. *Proc. Natl. Acad. Sci. U.S.A.* 97: 14632–7.
46. Lange S, Xiang F, Yakovenko A, et al. (2005) The kinase domain of titin controls muscle gene expression and protein turnover. *Science* 308: 1599–1603.
47. Ansved T. (1995) Effects of immobilization on the rat soleus muscle in relation to age. *Acta Physiol. Scand.* 154:291–302.
48. Ansved T, Larsson L. (1990) Effects of denervation on enzyme-histochemical and morphometrical properties of the rat soleus muscle in relation to age. *Acta Physiol. Scand.* 139:297–304.